Design and Performance of a Front End electronic ASIC for the OPERA Scintillator Target Tracker (Version-2)

S. Bondil[(1)], K. Borer[(2)], J. Boucrot[(1)], J.E. Campagne[(1)],
A. Cazes[(1)], M. Hess[(2)], Ch. de La Taille[(1)], A. Lucotte[(1)],
G. Martin-Chassard[(1)], L. Raux[(1)], J.P Repellin[(1)]

[(1)] LAL-IN2P3 - Univ. Paris-Sud - B.P. 34 - 91898 Orsay Cedex
[(2)] Bern University, Bern, Switzerland

Abstract

Multi-anode photomultipliers HM7546 are used to readout signal from the OPERA Scintillator Tracker [1]. A 32-channels front-end chip prototype accomodating the HM7546 has been designed at LAL. This device features a variable gain preamplifier to correct for multi-anode non-uniformity, an auto-trigger capability 100% efficient at a fraction of a photo-electron, and a charge measurement extending over a large dynamic range [0-80] photo-electrons. Procedures of validation have been defined and applied to an improved version of the ASIC, called Version-2. The conclusion is that this front-end chip meets the requirements as defined by the collaboration. The conducted studies also allowed us to identify several aspects of the ASIC that can be furhter improved in a future evolution of the chip.

Contents

1 Introduction

1.1 The OPERA experiment

The goal of the OPERA experiment, a massive lead/emulsion target, is to search for the appearance of $\nu_\mu \rightarrow \nu_\tau$ oscillations in the CNGS (Cern Neutrino to Gran Sasso) beam. It exploits nuclear emulsion for the unambiguous detection of the decay of the τ produced in ν_τ interactions. The detector is displayed in Fig. 1.1 and is being built on the basis of two supermodules. Each supermodule consists of a target-tracker section where the interaction takes place followed by a muon spectrometer, allowing muon identification as well as sign and momentum determination. The target-tracker section is composed of 31 planes of emulsion+lead bricks interpaced with scintillator tracker detector planes. These latter are used to identify the brick where the neutrino interaction took place in order to perform a precise scanning.

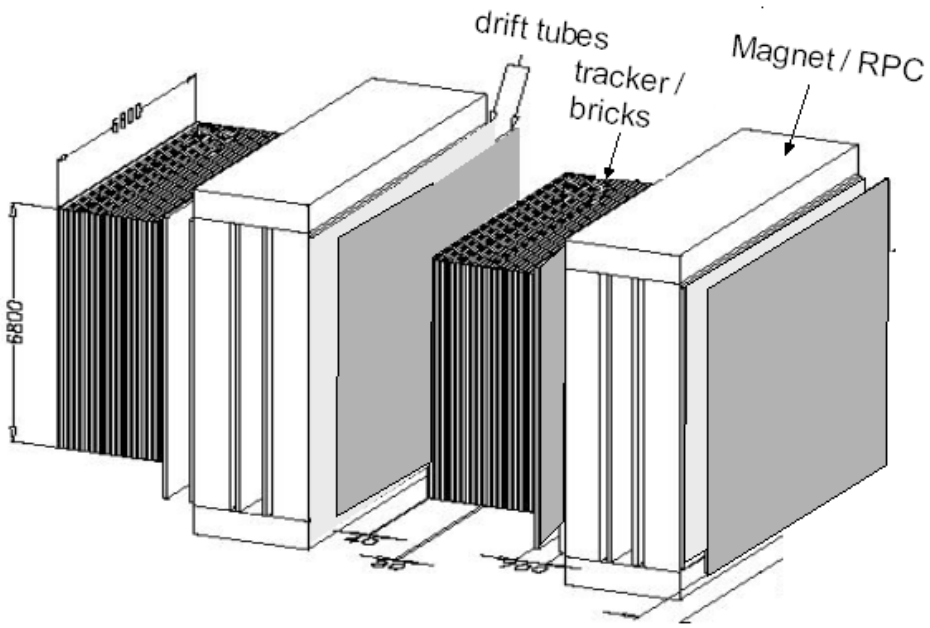

Figure 1.1: *View of the Opera detector*

1.2 The Scintillator Tracker and requirements on front-end electronics

A scintillator plane is shown in Fig. 1.2. It consists in four 760 cm-long modules in the X- and four in Y-directions. Each module is made of 64 extruded scintillator strips, 6.7 m length, 1 cm thich, 2.6 cm wide of rectangular cross-section. The scintillator strips are obtained by extrusion with a TiO_2 co-extruted reflective coating for better light collection. They are designed with an embedded wavelength-shifting fiber in the center of the strip and readout at both ends. Detector details can be found in Ref. [2].

The blue light emitted by each optically isolated strip is absorbed in the wavelength-shifting fiber and re-emitted into the green, before a transmission to photomultiplier tubes (PMT), as sketched in Fig. 1.3. The collaboration has decided to use multi-anode PM Tubes made by Hamamatsu, referrenced as H8804MOD. The PMT contains 64 independent channels, each of them covering a surface of 2.3×2.3 mm^2 and has two series of 12 dynodes. The output from each channel is provided with a gain ranging from 10^5 to 10^6. The readout electronics of this system consists of a multi-channel chip, which delivers a global auto-trigger as time information, and a charge proportional to the energy deposited in the scintillator.

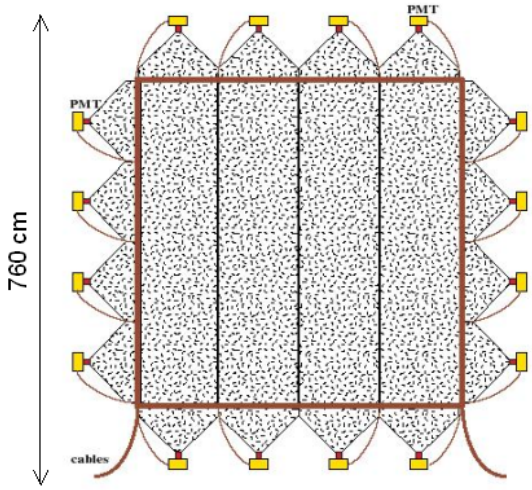

Figure 1.2: *A scintillator plane represented with the 64-channel PMT's used for the readout*

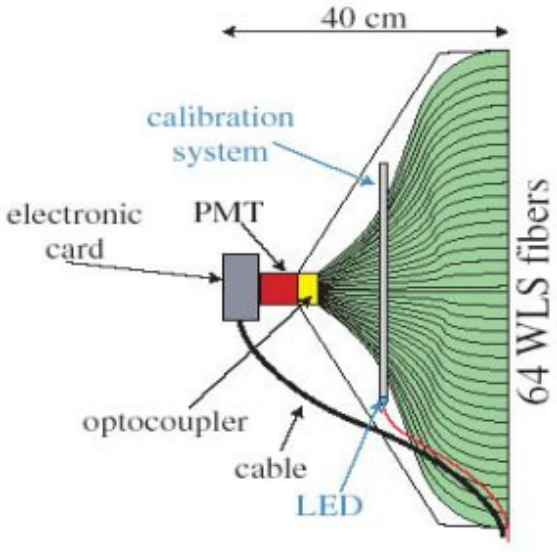

Figure 1.3: *Connection between scintillator module and a 64-channel PMT*

The emphasis has been put on the detection of particle at minimum of ionsation (MIP). Typically, particles traversing the scintillator at the center of the strips, deposit around 6 photoelectrons. Fig. 1.6 shows the light yield as function of the distance from the impact to the PMT. This distance is ranging from 1 to 6.5 m with fibers attenuation length is typically above 700 cm. These characteristics impose strong requirements on the trigger capabilities, and a 100% trigger efficiency is required as low as a 1/3rd of photoelectron, which corresponds to about 50 fC at the anode for a PMT gain of 10^6. This ensures that a 100% trigger efficiency is reached for particules at minimum ionisation. A dynamic range of the charge measurement up to about 100 photoelectrons is required.

A large bandwidth is necessary for a good matching with a fast PMT signal shape. Besides, studies in Ref. [4] and ref. [5] show that a gain variation by of a factor 3 occurs between the different channels of the same PMT, as seen in Fig. 1.5. In order to compensate this large difference between channels, the front-end electronics must be equipped with an adjustable gain

system, directly incorporated in the preamplifier stage. This allows good integration density and delivers a signal of identical range to the fast and slow shaper of every channel.
To avoid cross-talk between anodes in the detector, the preamplifier must have low input impedance. We aim at a front end approaching a signal to noise ratio of 100, which would allow an autotrigger at a level of 1/16 p.e. The aim is to ensure a 100% trigger efficiency at a 1/3rd photoelectrons, i.e. at 8 sigmas.

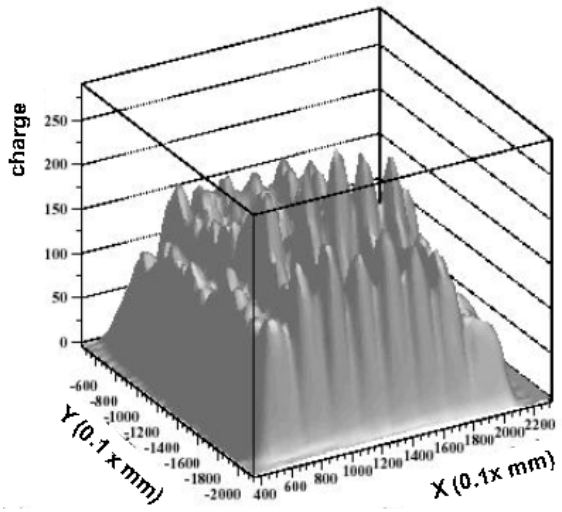

Figure 1.4: *Gain variations as seen for the 64 channels of the H7546 PMT by Hamamatsu*

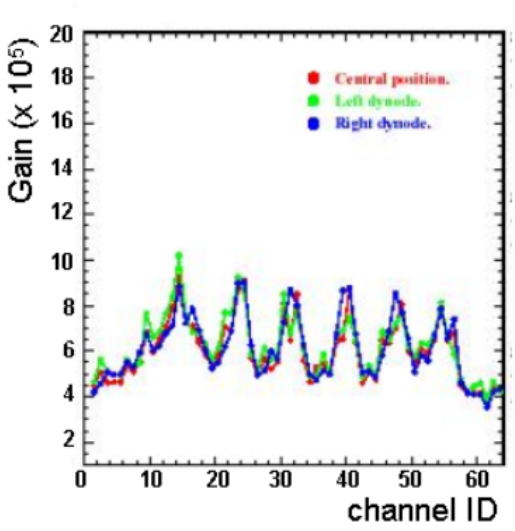

Figure 1.5: *Gain variations as seen for the 64 channels of the H7546 PMT by Hamamatsu*

The LAL shares the responsability with Bern University to provide the front end electronics for the 992 PMT's used to readout signals from the scintillator Target Tracker of OPERA. While LAL designs the ASIC's used to readout signal from the scintillator Target Tracker, Bern university designs the mother Boards that is implemented on the FE chip.

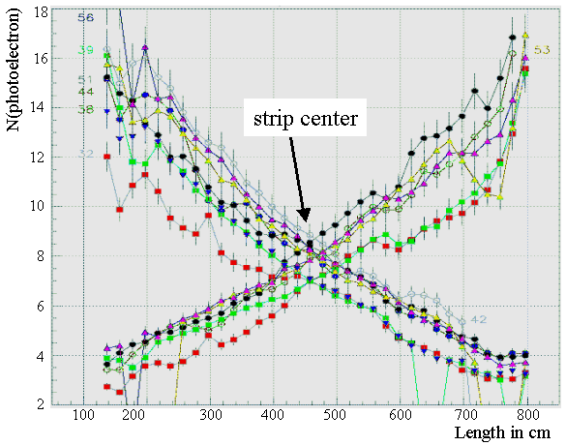

Figure 1.6: *Light yields at both ends of a scintillator strip module for different choices of scintillator fibers. In all cases, a MIP corresponds to more than 6 photoelectrons*

2 Design of the Front-End Electronics

2.1 ASIC functionalities

Based on the AMS 0.8μm BiCMOS technology, a complete chip with 32 channels and 2 extra test channels has been designed by the LAL group to fullfill the Target Tracker requirements. A view of the 32 channel chip is shown in Fig.2.7.

Each channel contains a variable gain preamplifier, based on a current mirror architecture, that feeds both the slow and fast shaper channels. The gain amplification extends from 1 to 2.875 by adding to the intial input respectively 1, 1/2, 1/4 and 1/8 times the input signal with a resolution of 4 bits (each current mirror branch being affected to a weight 1, 1/2, 1/4, 1/8 via adjustable resistor). This adjustable gain preamplifier is connected on one side to a fast shaper ($\tau_{\text{peak}} = 10$ ns, G ≈ 20) to provide auto-trigger, and on the other side to a slow shaper ($\tau_{\text{peak}} = 120$ ns, G ≈ 1) for an accurate charge measurement. The fast shaper goes in a comparator and a OR of all the comparator outputs gives the trigger decision; the threshold is global for the 32 channel so a mask register allows to disable a noisy channel. Upon a trigger decision, the slow shaper signal is captured by a track and hold system where the charge is stored in a 2 pF capacitance. The 32 channels outputs are multiplexed with a readout frequency of 5 MHz, which gives a total readout time of 6.4 μs (32*200 ns). A channel architecture is presented in Fig. 2.8.

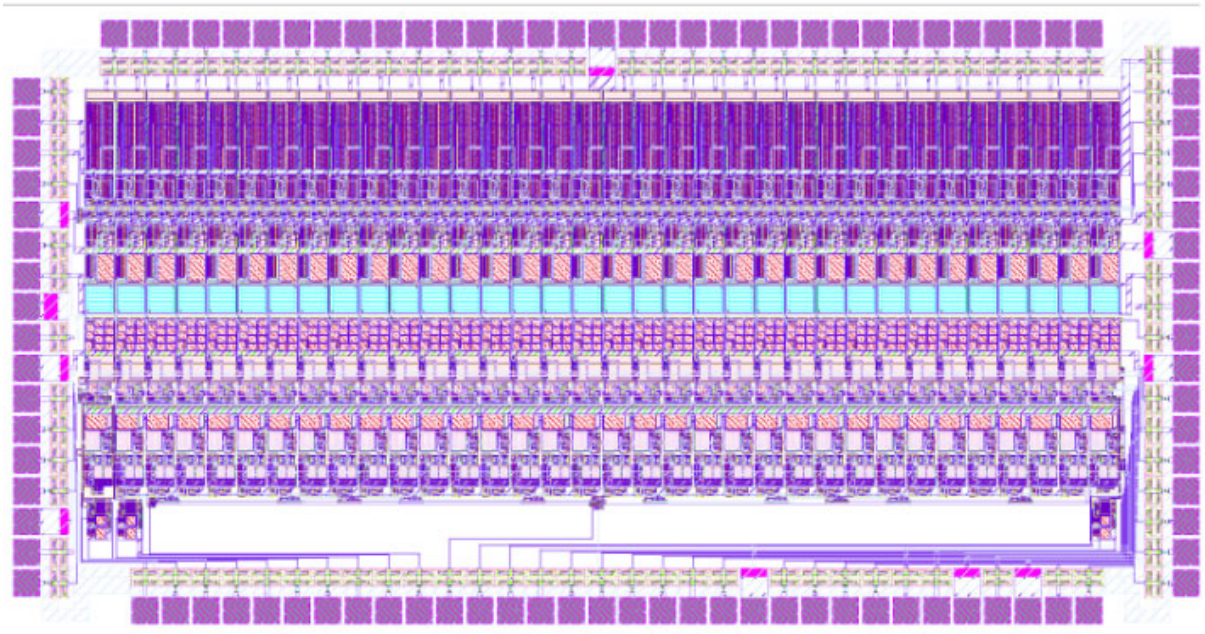

Figure 2.7: *View of the 32 channel chip design. Total area is about* 10 mm^2

Two other dummy channels (Ch0 and Ch33) were added and used as test channels: the first

one (Ch0) provides the DC references and the second one (Ch33), powered separately, allows intermediate output measurements. The total power consumption of the chip is about 0.25 W (8 mW per channel). The chip area is 10 mm^2 and it is packaged in a QFP100 case.

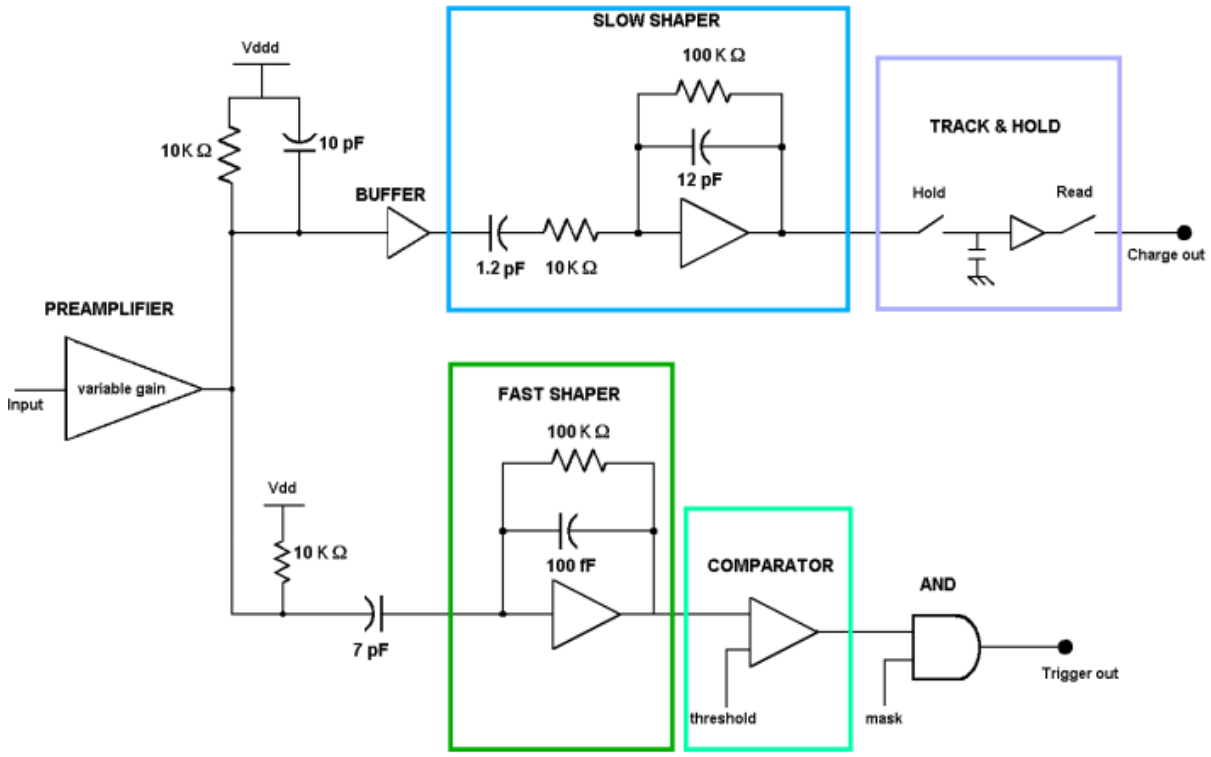

Figure 2.8: *Schematics of a single channel*

2.2 Preamplifier architecture

The topology for PMT readout is based on current mirroring. The schematic of the preamplifier is presented in Fig. 2.9. Due to the polarity of the pulse current at the anode output of the detector, and considering that in AMS BiCMOS 0.8 mm technology, the only PNP transistor available is a lateral one with poor β, a PMOS transistor is used as input transistor.
The input stage has a cascaded current mirror structure with unity gain. This design allows a better current linearity and a higher output resistance. Variable gain system is implemented by adding switchable other current mirrors with various gain (1+[1, 0.5, 0.25, 0.125]). The detector current can be here multiplied up to close a factor three. This stage is followed by a second NPN unity gain mirror current in order to inverse the shape polarity and to send the signal separately to the fast and the slow shapers.
The input impedance is given by:

$$Z_{in} = (g_{m1} + g_{mc1})/(g_{m1} \times g_{mc1}) \approx 500\Omega$$

After these two mirrors, the current is converted in a voltage signal in a RC cell with a time constant of 100ns. The global transfer function is given by:

$$\mathrm{V_{out}/I_{in}} = -\mathrm{R_f}/(1 + \mathrm{sR_fC_f}) \quad \text{with } \tau_{\mathrm{peak}} = \mathrm{R_fC_f} = 100 \text{ ns}$$

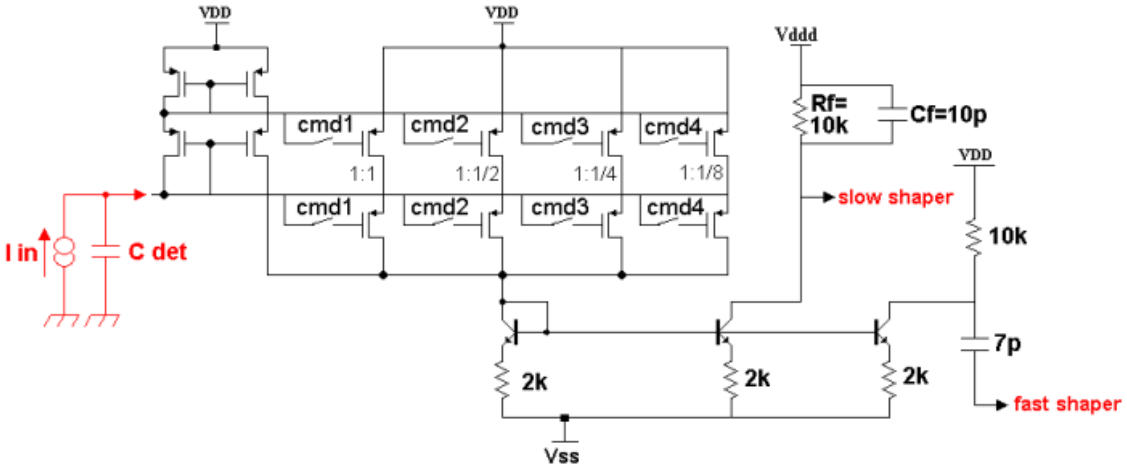

Figure 2.9: *Preamplifier current-mirror architecture*

2.3 Slow and fast shapers

Each channel contains a preamplifier followed in parallel by a slow and a fast shaper as presented in Fig. 2.8.

2.3.1 Slow shaper

To obtain the charge information of the particle interaction with the detector, the current pulse is converted in voltage step by the preamplifier and then slightly amplified and filtered by a CR-RC shaper. This shaper is AC coupled to the preamplifier by a 12 pF capacitor followed by a 10 kΩ resistor. It is built around a conventional amplifier with a RC feedback, which sets the time constant of the filter. This design allows a good linearity over the whole dynamic range of the signal.

Another important function of the shaper is to optimize the S/N ratio. In our system, the parallel noise predominates, so fast shaping is recommended. But the shaper is the input to the future sampling stage, which can have some jitter from physics sources. To satisfy these

two antagonist needs, a shaping time of 120 ns was chosen. Fig. 2.10 shows the slow shaper architecture.

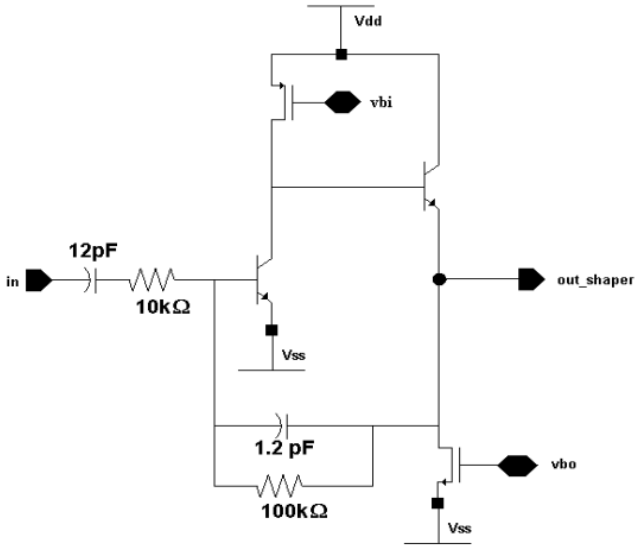

Figure 2.10: *Slow shaper architecture. Resistor and capacitors values are the actual values of the present design*

The amplifier, with a structure based on a simple transimpedance configuration, has a gain band width GBW=3.5 GHz, an open loop gain G_0=560 and a dominant pole at w_0=20 MHz. as shown in Fig. 2.11. The shaper transfer function is given by:

$$H(s) = -sR_2C_1/(1+sR_1C_1)(1+sR_2C_2) \text{ with } R_1C_1 = R_2C_2 \ = t \ = 120 \text{ ns}$$

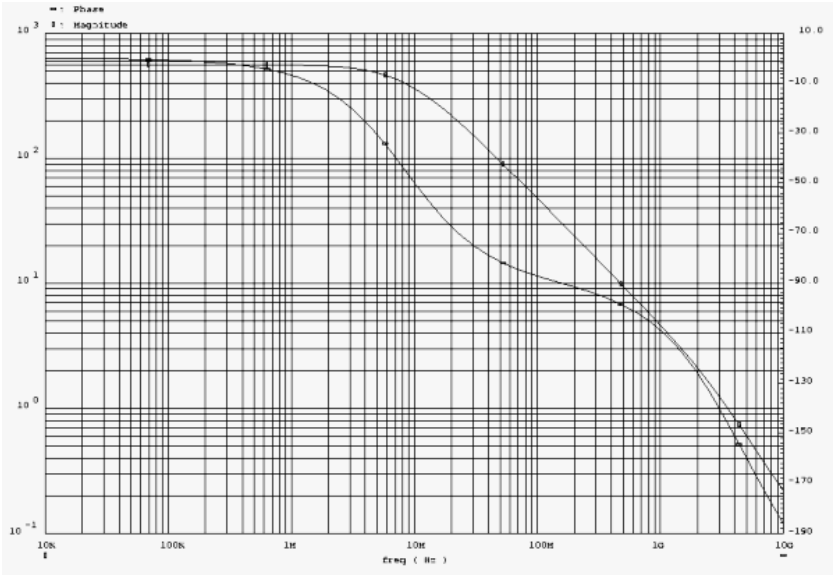

Figure 2.11: *Slow shaper open loop Gain as function of input rate in Hz (simulation)*

2.3.2 Fast shaper

To obtain the time information of the particle interaction with the detector and the Track and Hold system, the current pulse is converted in voltage step by the preamplifier and then highly amplified by a fast shaper before to be injected in a comparator. It is built by a bipolar amplifier with a R_fC_f feedback which sets a time constant of 10ns for the filter. A very high gain is implemented (around 20) to give the possibility to this stage to easily trigger a comparator. As mentioned before, the system is able to be trigged on 1/16 of a photoelectron; a simulation of the whole channel gives a S/N ratio of 118 at this fast shaper output with the mirror current preamplifier. Fig. 2.12 shows the fast shaper architecture.

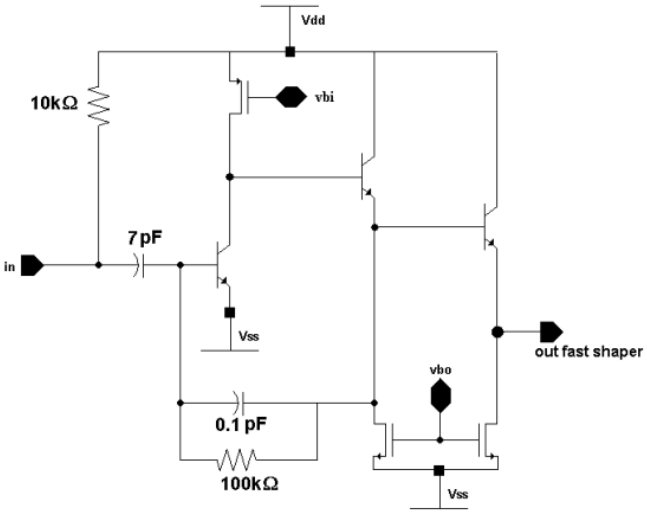

Figure 2.12: *Fast shaper architecture.*

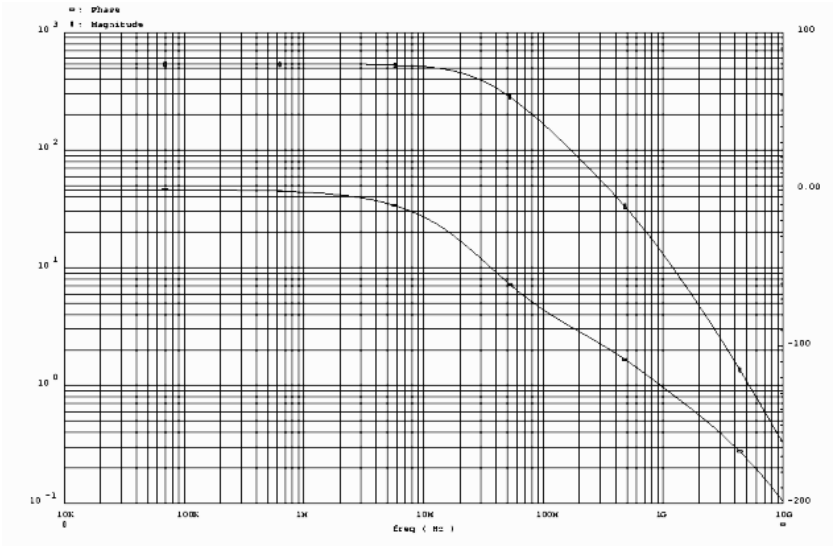

Figure 2.13: *Fast shaper open loop Gain as function of input rate in Hz (simulation)*

The amplifier has a gain band width GBW = 5 GHz, an open loop gain G_0= 540 and a dominant pole at w_0= 20 MHz as shown in Fig. 2.13.

2.4 Signal acquisition

The preamplifier and the slow shaper, seen in the previous paragraphs, followed by a basic sample and hold system, compose the charge analysis chain. The schematic of this sample and hold is given in Fig. 2.14. The maximum of the slow shaper output signal is stored in a 2 pF capacitor. When a trigger signal occurs, all the capacitors are read sequentially through a shift register made by D-flip-flop.

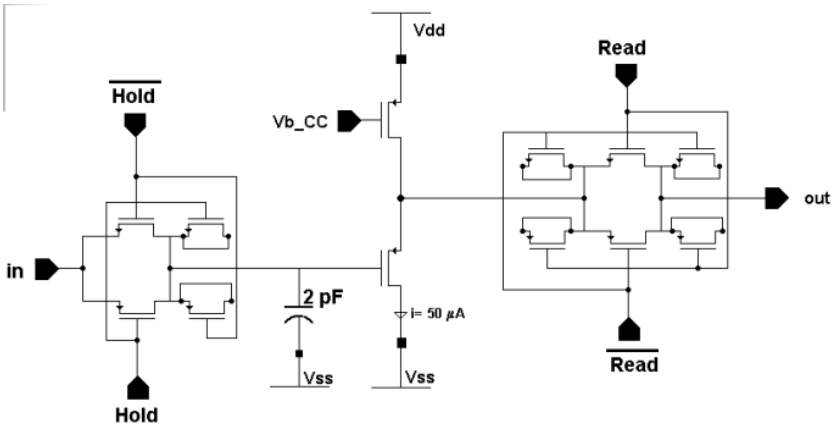

Figure 2.14: *Signal acquisition and readout*

2.5 Trigger

The trigger path is composed of the fast shaper seen in the previous paragraph, followed by a comparator. The schematic of this comparator is given in Fig. 2.15.
The input stage of this comparator is designed by a bipolar differential pair in order to minimize the offset. With a low offset comparator and a high gain in the shaping just before, a common threshold can be used for all channels. All the comparators outputs are "ORed" to give a trigger for acquisition. A mask register has been added in order to disable a too noisy channel.

2.6 From Version 1 to Version 2 ASIC

The fisrt version of the ASIC has been extensively tested and the results reported in a note [7]. Although Version 1 architecture is remained unchanged, some modifications have been applied to the first version chip.
First, a comparator over-current in version 1 has been cured by separating the analog and digital supplies. Output inverter transistors have been re-sized and some resistors have been added to limit the current in the branch.
Then, a new power supply distribution has allowed a reduction of voltage drop accros power

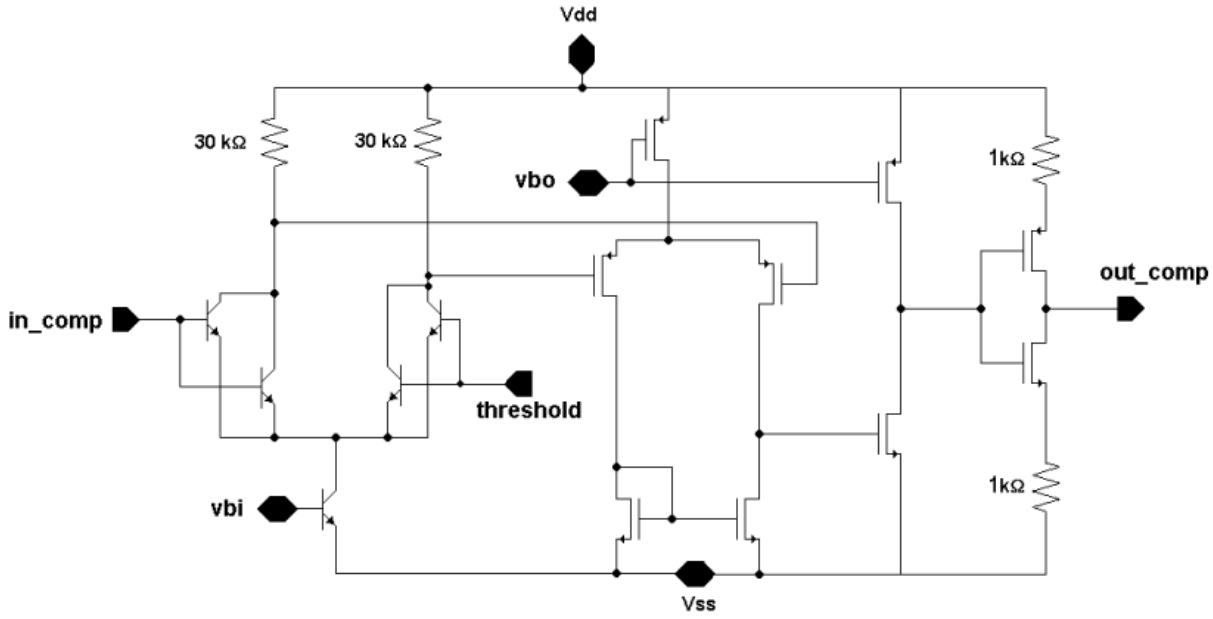

Figure 2.15: *Trigger architecture*

supply lines. This has been done while keeping unchanged the chip pinout.
Eventually, shapers parameters have been tuned. Slow shaper peaking time has been raised from 100 ns to 120 ns and slow shaper gain has been adjusted to decrease the gain of 170 mV/pC to 140 mV/pC (ie: from 27 mV/p.e. down to 22 mV/p.e.).

3 Performance of the FE electronics ASIC

Performances have been measured using a test card and test equipment designed and constructed by Bern University. Measurements performed on Version-1 are reported in an OPERA internal note [7] and have lead to the production of an improved design, called Version-2. We focus here on the understanding as well as on the measured performance in view of the ASIC validation for physics use. Note that, in the following, an input charge of 1 photoelectron corresponds to 160 fC, assuming a photomultiplier gain of 10^6.

3.1 Variable gain preamplifier

The variable gain preamplifier is aimed at correcting for non-uniformity seen with the multi-anode photomultiplier tubes H7546. Those channel-to-channel non-uniformities have been measured in Ref. [4] and [5], may be as high as 300%, see Section 1.2. They define the actual requirements on the preamplifier.

There is no direct access to the individual preamplifier output in the chip, so that measurements have to be performed externally on a test channel (channel 33). Preamplifier gain is found to be 60 mV/pC (10 mV per photoelectron) with a peaking time of 30 ns for a null gain correction (gain 1). This is consistent with the expectation from the design settings.

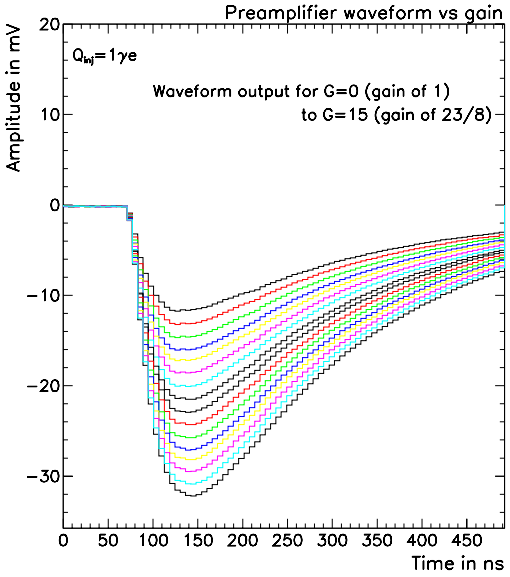

Figure 3.16: *Preamplifier Output waveform for different input charges in test channel 33*

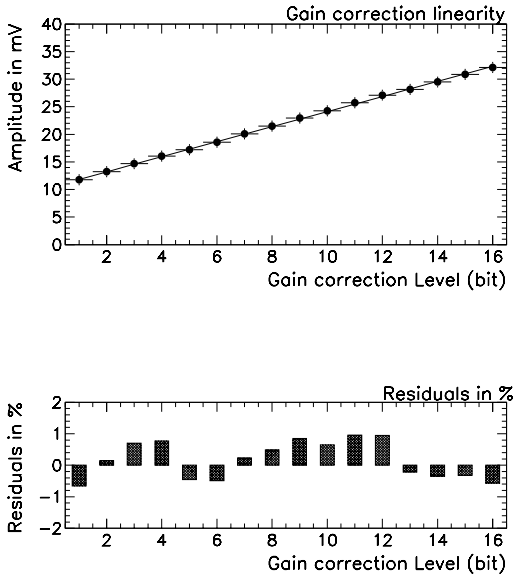

Figure 3.17: *Preamplifier gain linearity: residuals wrt straight fit line computed on channel 33*

The four (current mirror) switches allow to set 15 amplification levels of correction per channel, ranging from 1 time the input charge to (1+15/8) times the input, by steps of 1/8. All levels of

gain amplifications from 1 to 2.875 have been applied to an input signal corresponding to 1 p.e. The output waveforms of an individual channel are shown in Fig. 3.16 for each setting. The 16 possible levels of correction are proved to be reliable and residuals (computed with respect to a linear fit) are found below the percent level over the full range of correction, as seen in Fig. 3.17.

3.2 Auto-trigger channels

Every channel of the chip has the capability to integrate and store the charge upon a trigger decision. Triggering is ON as soon as at least (any)one of the 32 fast shaper channels detects a signal above a certain threshold.
While emphasis has been put to ensure that trigger efficiency is 100% as low as $1/3^{rd}$ of photoelectron, it is also desirable to avoid large threshold offsets among the 32 channels. These constraints drive the series of tests performed on the chip.

3.2.1 Fast shaper characteristics

Similarly to previous section, there is no direct access to individual fast shaper outputs in the chip. Measurements are therefore made on the test channel (channel 33) where intermediate outputs have been designed. Signal is then readout externally. Characteristics of fast shaper output waveforms are illustrated in Fig. 3.18 where they are represented for all gain correction settings defined at the preamplifier stage.

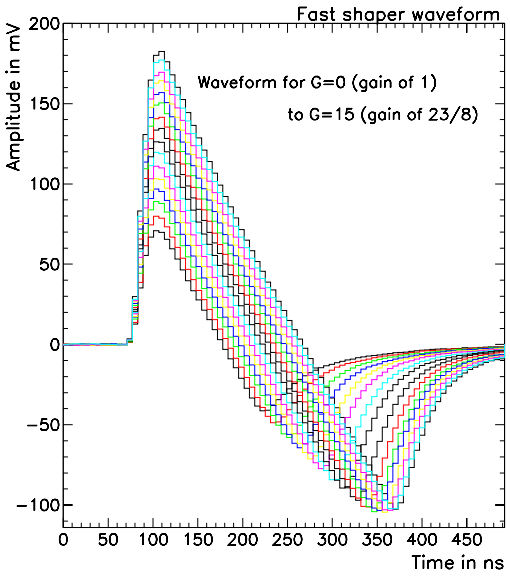

Figure 3.18: *Output waveform measured at the Fast Shaper for a set of gain correction ranging from 1 to 2.875. Note that fast shaper characteristics are only directly accessible via the test channel 33, readout externally (which results in the observed slew rate). Characteristics are a gain of 880 mV/pC and a peaking time of 30 ns*

A gain of 880 mV/pC (140 mV/p.e.) is measured for a null preamplifier correction for a peaking time of 30 ns. The gain linearity has been checked over the full range of correction and found

reliable. Fig. 3.18 also displays clearly the slew rate due to an external readout of the signal. Fast shaper pedestal is about 0.9 V.

3.2.2 Comparator and time walk

Fast shaper ouputs are compared to an adjustable threshold and ORed at the comparator stage. In the case where one channel at least is above the threshold, a trigger decision is taken and signal is sent to store signals out of slow shapers 100 ns later.
The output signal from the comparator is a 5 V signal as seen in Fig. 3.19. The trigger rise time only slightly depends on the input charge magnitude, since a factor 100 increase in the input signal only results in an 10 ns delay in the trigger desicion. Given the attenuation factor in the 6 meter long scintillators, this delay is acceptable from the physics standpoint (no precise time measurement is needed on the scintillator ends). Fig. 3.19 shows the corresponding time walk for input charges of 1/3 of p.e. and 30 p.e. respectively.

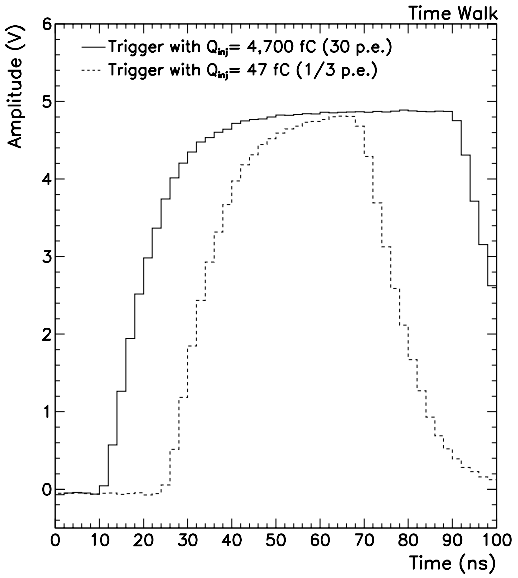

Figure 3.19: *Time walk for the output trigger signal. Here trigger response is shown for two injected charge of 1/3rd photoelectron and 30 photoelectrons in channel 01*

3.2.3 Trigger efficiency: S-curves

Trigger efficiency has been measured as function of the input charge for each individual channel. Obtained S-curves are displayed in Fig. 3.20 and show that the chip is fully efficient for input charge as low as 35 mV ie: 1/4th of photoelectron. The 50% trigger efficiency thresholds distribution, measured among all 32 channels, is represented in Fig. 3.21. The spread is shown to remain around 14 mV ie: 0.10 photoelectron. It is mainly due to the fast shaper. The comparator contribution is estimated at around 1 mV and is negligible compared to the previous source.

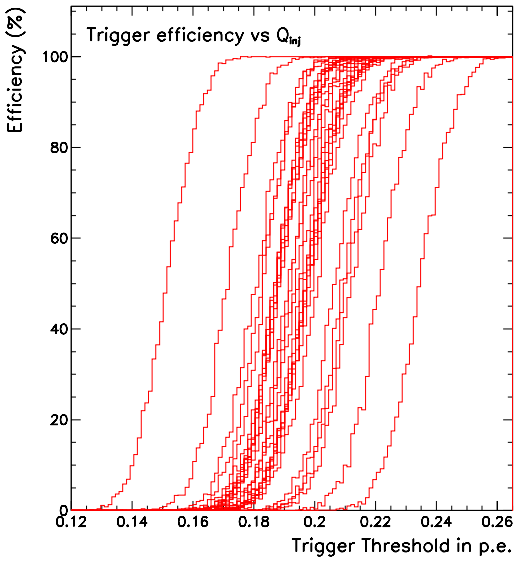

Figure 3.20: *Trigger efficiency (S-curve) as function of the input charge for the 32 channels*

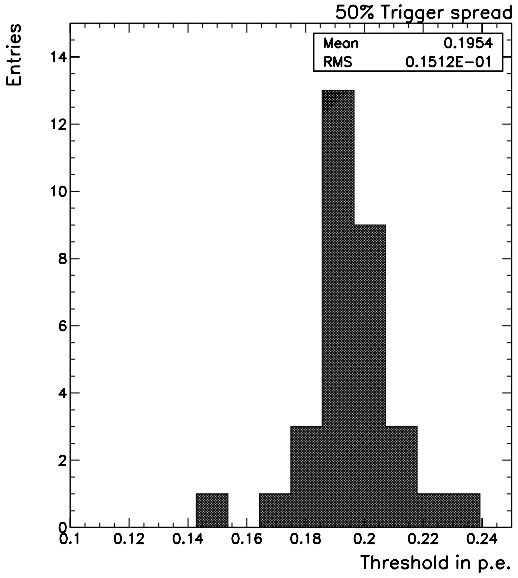

Figure 3.21: *50% trigger efficiency threshold dispread for all 32 channels*

Preamplifier gain correction levels may have some effect on trigger thresholds. To assess such effect, S-curves have been measured in a single channel by keeping constant the injected charge while increasing the preamplifier correction settings from a gain 1 to a gain 2.875, all other channels being set to a null correction. A sizeable dependence is found as illustrated in Fig. 3.22, where 50% efficiency trigger thresholds decrease from 1/5th photoelectron to about 1/10th photoelectron as the (preamplifier) gain settings goes from 1 to the maximal gain.
If one repeats S-curve measurements on the same single channel, all other channels being this time set to the maximal gain correction, an average of -0.1 photoelectron reduction of the 50% trigger efficiency thresholds is observed.

3.2.4 Fast shaper Noise

Noise RMS can be indirectly extracted from the S-curves using the slope at the 50% trigger efficiency point. Distribution for all 32 channel noise values are shown in Fig. 3.23. An average value of 1.3 mV is found for a fast-shaper amplification factor of 140 mV/p.e. and a null gain correction.

This result corresponds to about 1% photoelectron and is consistent with the expectations and much lower than the 1/3rd photoelectron threshold used for physics purposes. Direct noise measurement performed on the fast shaper test-channel confirms this results. 1.5 mV rms for a null gain correction and 2.8 mV for a maximal gain are found on the test channel 33, corresponding to an input charge of respectively 1.9 fC at zero gain and 1.4 fC at maximal gain.

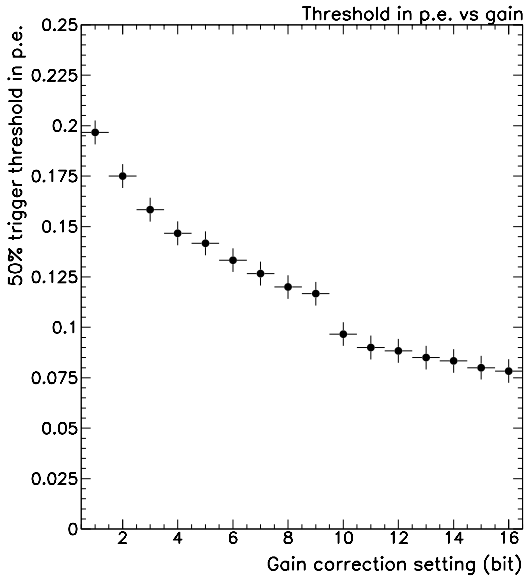

Figure 3.22: *Trigger threshold for a single channel at 50% efficiency as function of the gain correction*

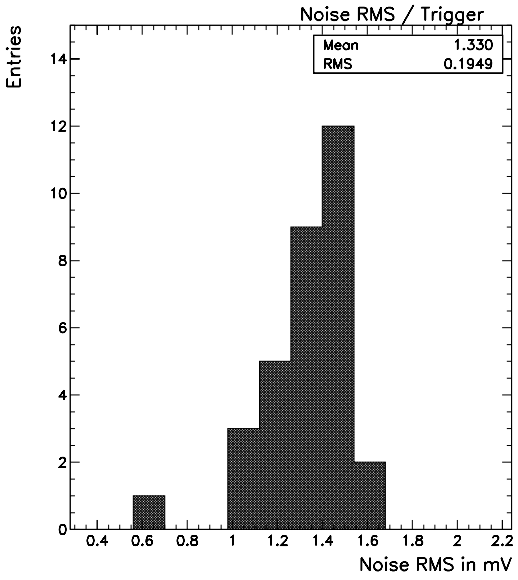

Figure 3.23: *Noise RMS for all 32 trigger channels exctrated from the 32 channel S-curve slope measurements at the 50% trigger efficiency point*

As the gain is about 1.4 times greater for the test channel than for channel 1-32 that are used for the measurement, we conservatively quote noise value of 1.5 to 4 mV for channel 1 to 32. These results are consistent with indirect determination from the S-curves.
All results hence prove that electronic noise is not an issue in the working conditions of the OPERA Target Tracker.

3.3 Charge measurement channels

3.3.1 Gain correction

Fig.3.25 displays the waveform output of a single channel slow shaper for an input charge of 2.5 photoelectrons and all different gain correction settings. For every channel the gain corrections, that are applied to the input signal and transmitted to both slow and fast shapers, is found to be functionnal. A linear fit applied on the measurements shows a good (χ^2/d.o.f = 0.1) while residuals, computed with respect to the fit result, show that no discrepancy above 1% are found over the full range of gain amplification. This is shown in Fig. 3.25 for the 16 levels of gain correction settings.

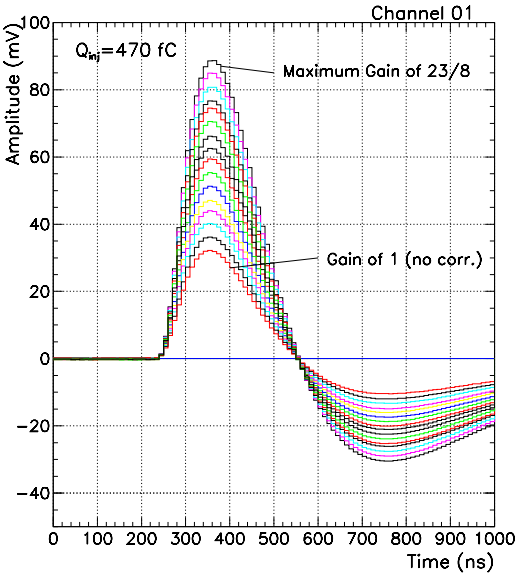

Figure 3.24: *Variable gain preamplifier corrections. The four bits allow a correction of +1,+1/2,+1/4 and +1/8 for a maximum gain amplification of 2.875*

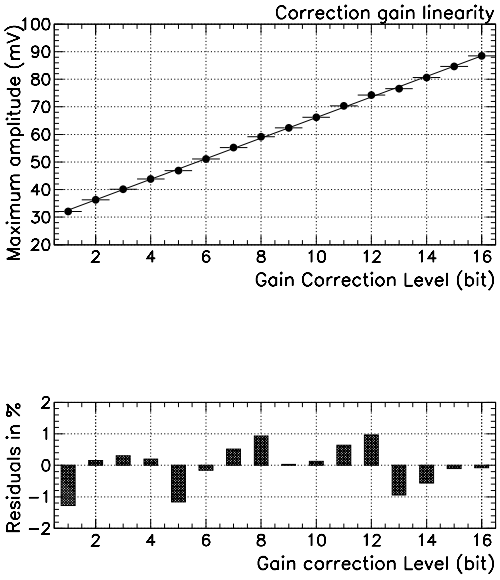

Figure 3.25: *(top) Linearity of the correction factor as function of the bit settings. (bottom) Residuals computed wrt the fit results*

3.3.2 Slow shaper characteristics

For a null gain correction at the preamplifier stage, the averaged maximum amplitude, V_{max}, in the charge measurement channel is 130 mV/pC (ie 20 mV per p.e.). Fig. 3.26 displays the 32 channel slow shaper output V_{max} for a 2.5 photoelectron input charge as function of the channel ID while Fig. 3.27 shows corresponding V_{max} distributions. Two configurations, representing the extreme cases, are considered: in the first case, all channels are set to a null gain correction (gain 1); in the second, all channels are set to the maximal gain correction . The ratio for the average V_{max} is found to be 2.911, consistent with the maximal value of 2.875.

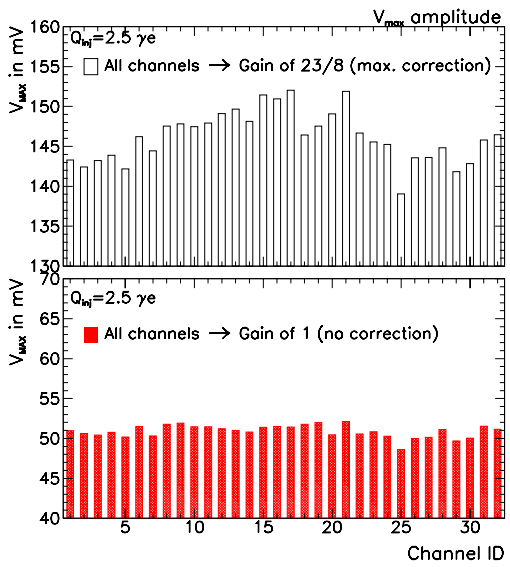

Figure 3.26: *Gain as function the channel ID for both a null (bottom plot) and a maximal gain correction (top plot) for an input charge of 2.5 p.e.*

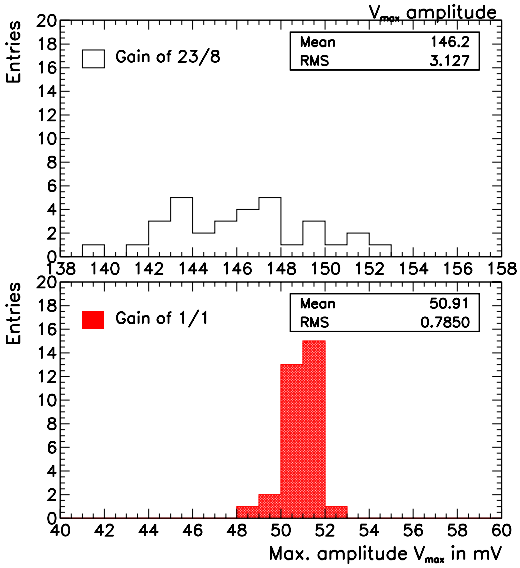

Figure 3.27: *Maximum amplitude V_{max} distribution for an input charge of 2.5 photoelectrons and a minimal (bottom) and a maximal gain correction*

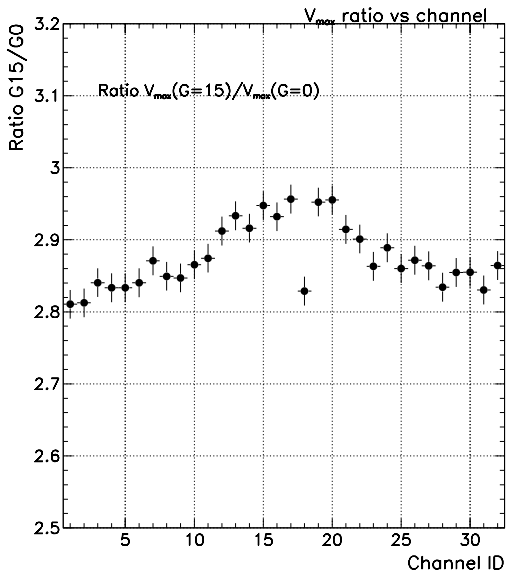

Figure 3.28: *Ratio* $\mathrm{V_{max}(G = 23/8)/V_{max}(G = 1)}$ *for all 32 channels computed as the maximum gain correction over the minimum gain correction level*

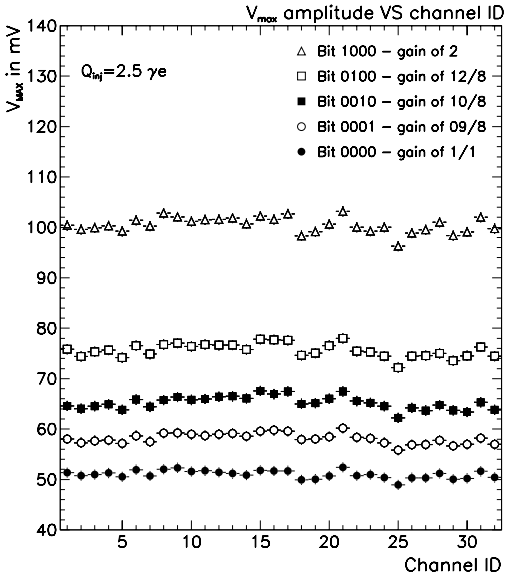

Figure 3.29: $\mathrm{V_{max}}$ *for all 32 channels computed for 4 levels of gain correction, corresponding to the 4 bits settings, 0001, 0010, 0100 and 1000*

Waveform peak amplitudes V_{max}, represented in Fig. 3.27, show significantely different spreads fot both gain corrections. For a null gain correction settings, a spread of 6 mV is found among the 32 channels, while for the maximal correction this value reaches 16 mV. One has to notice that both values however represent a significant improvement with respect to the previous version of the chip, which had a spread of 40 mV.

Further investigations have shown the larger spread obtained for maximal gain correction settings is affected by problems with some levels of corrections, that are not properly functionnal for certains channels. These channels have been identified and such effect is shown to affect the gain correction at maximum by 2% of the total input charge at the maximum gain, as seen in Fig. 3.28. We therefore conclude that no significant degradation is seen for the gain correction.

A thorough test the current mirror architecture has been conducted in order to check wether this effect was affecting any particular individual mirror branch. For this purpose, all of the four correspondig but was turned ON/OFF and the gain measured. Fig. 3.29 shows the gain magnitude as each of the four current mirror alone (with weight 1/8, 2/8, 4/8 and 8/8) is used to correct the initial signal for the 32 channels. No deviation exceeding the 2% level is seen among the four branches. We therefore conclude that no structural flaw affects the mirrors and that the gain correction is fully functionnal up to the nominal 2.875 maximal gain correction.

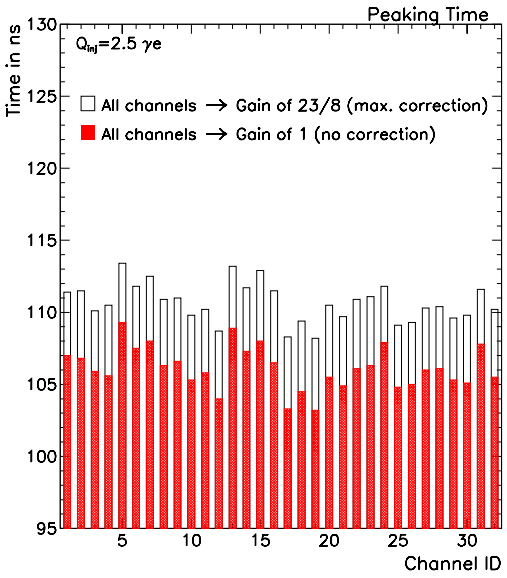

Figure 3.30: *Peaking Time measured for an input charge of 2.5 p.e. as function of channel ID when all channels are set to a null gain (lines) and to a maximal gain corrections (plain)*

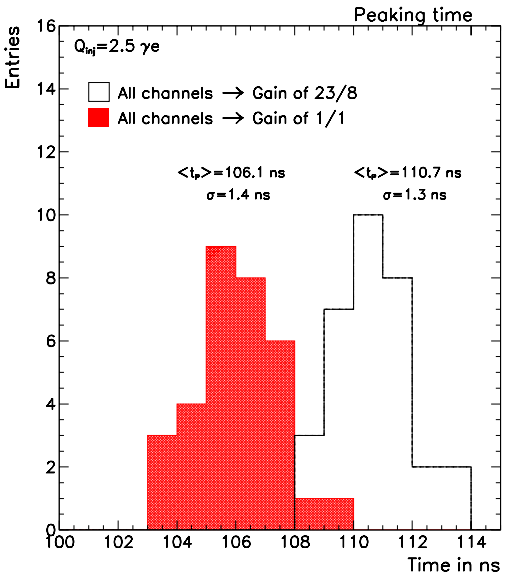

Figure 3.31: *Peaking Time distributions for a 2.5 p.e. input charge when all channels are set to a null gain or a maximal gain correction*

3.3.3 Slow shaper peaking time

The average peaking time computed on the 32 channels is 106 ns for an input charge corresponding to 2 photoelectrons. This is true when all other channels are set to a null gain correction at the preamplifier stage. Actually, the peaking time slightly increases to 111 ns as all channels are set to a maximal gain correction. Measurements are reported as function of the channel ID in Fig. 3.30.
Measurement spread is shown to be stable, with a 6 ns dispersion in both cases, as seen in Fig. 3.31. For input charges above 90 photoelectron, where saturation effects become significant, the offset does not exceed 10 ns in total.

3.3.4 Pedestal (V_{DC})

Pedestals are given by V_{DC} voltages, and have been measured for each individual channels. V_{DC} values are displayed as function of the channel number in Fig. 3.32 for both a null and the maximum preamplifier gain correction levels. For a null gain, the V_{DC} average is about 1,770 mV with a 30 mV total spread, corresponding to about 1.5 photoelectron. V_{DC} values are shifted towards higher values as the preamplifier gain corrections are set from the minimum to the maximum gain. Indeed the average V_{DC} value goes from 1,770 mV to 1,787 mV, as seen in Fig. 3.33. Gain correction settings does not affect in a visible way the distribution spread.

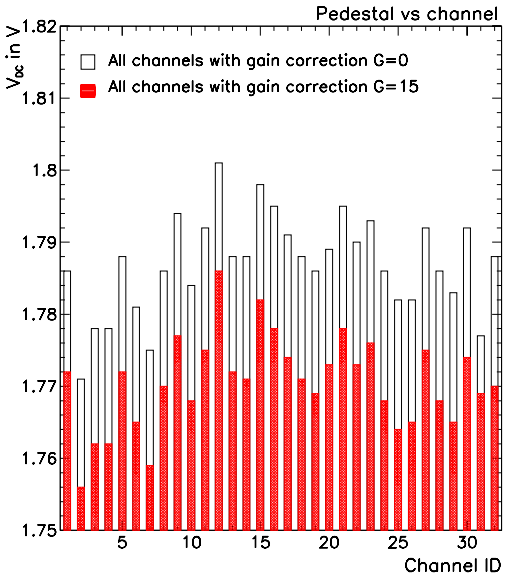

Figure 3.32: V_{DC} *measured for 32 channel for both a null gain and a maximal gain correction at the preamplifier stage)*

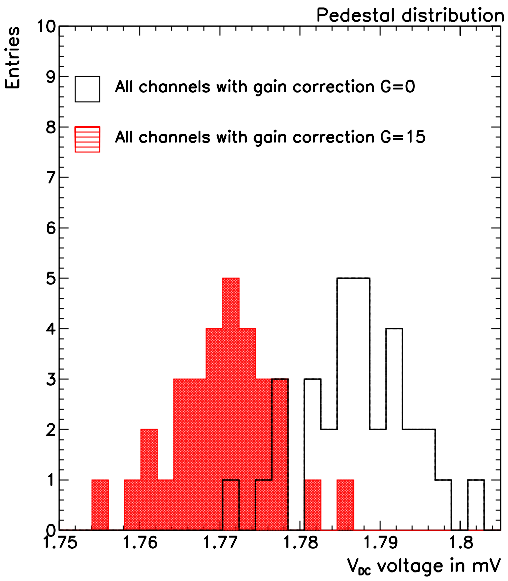

Figure 3.33: V_{DC} *distribution measured for 32 channels for both a null gain and a maximal gain corrections)*

This spread comes from two identified sources, about 50% from the slow shaper, and 50% from

the Track & Hold buffer and may be taken care of by appropriate offline corrections.

3.3.5 Response linearity

Response linearity is an important feature and stringent constraints are set by physics requirements. What matters most in Opera is however the precise determination of small input charges (MIP) for tracks reconstruction and muon ID.
The response linearity has been assessed as function of the input charge from 0 to 90 photoelectrons. No deviation above 2% is seen over the full [0-75]p.e. range, as it appears in Fig.3.34 and Fig. 3.35. However saturation phenomenon results in sizeable effects for charge above 75 p.e., with a 6% effect at 80 photoelectrons. One notices a slight degradation of the performance as one goes from channel 01 to channel 32 in the chip. The value at which saturation effect becomes significant indeed decreases regularly with higher numbered channels.

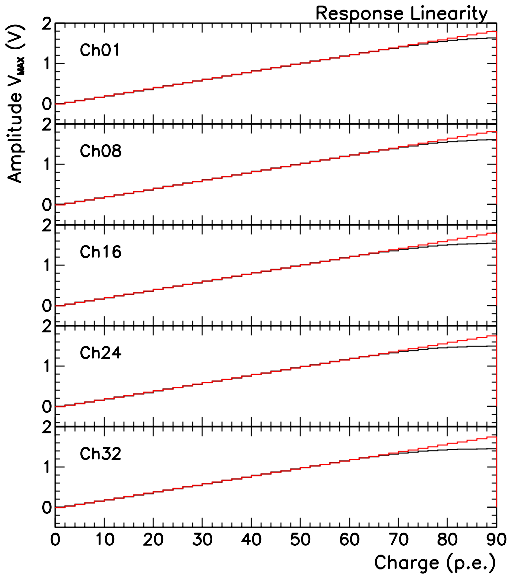

Figure 3.34: *Response linearity in the charge measurement as function of the input injected charge for channel 01, 08, 16, 24 and 32*

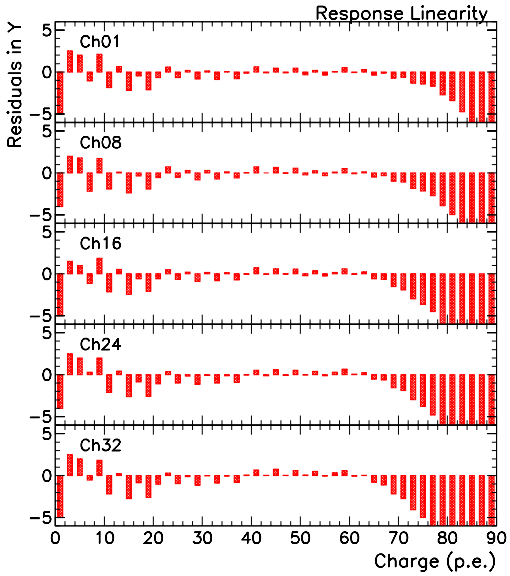

Figure 3.35: *Response linearity residuals as function of the injected charge for channels 01, 08, 16, 24 and 32*

The conclusion is that over the range [0,75] photoelectrons, indivudual response is linear to better than 2%, which fullfills the Target Tracker requirements. Regarding the higher part of the dynamic range, the place at which the saturation effect becomes significant is sensitive to the supply voltage V_{dd}. The tuning of this voltage allows us to improve the response linearity up to 100 photoelectrons if needed. This is obtained by increasing the supply voltage V_{dd} from the present setting of 4 V to about 5 V. The choice of the AMS BiCmos technology makes this adjustement possible up to $V_{dd} = 7$ V with no performance degradation. Figure 3.36 illustrates

the extended dynamic range for three different V_{dd} values.

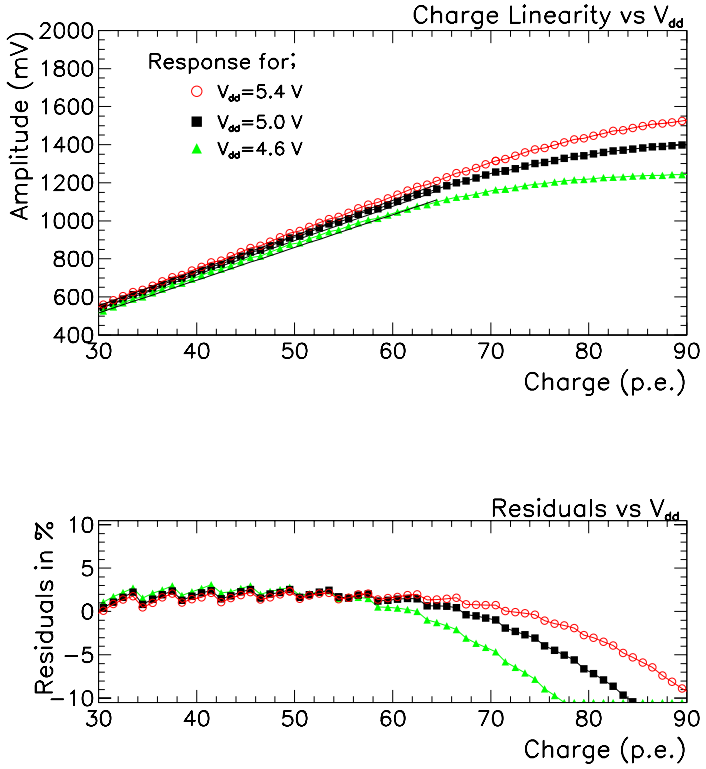

Figure 3.36: *Charge linearity of a single channel for three different settings of* V_{dd} *over the full dynamic range [0,90]p.e.*

3.4 Cross-talk

Cross-talk can affect the physics input to the ASIC. Indeed, such effects have been known to be non-negligible for the multi-anode PMTs used for the OPERA Target Tracker. Measurements reported in Ref. [5] for the LHCb experiment show that the magnitude of this "physics" cross-talk between 2 adjacent channels may be as high as 2-3%. This sets a reference number with which we have to compare such effects that can occur in the present ASIC.
Two kinds of cross-talk can affect the charge measurement by an individual channel in the present chip. The first kind of effect is due the coupling between the trigger channel and the charge measurement channel. The second source comes from the cross-talk among neighboring channels. The magnitude of such effects have been assessed in both cases.

3.4.1 Trigger-Charge crosstalk

Trigger-charge cross-talk effects are illustrated on Fig. 3.37, which shows the distorsion on a charge measurement for the channel with the injected charge as well as for its first neighbor. The injected charge is 1 photoelectron. The digital signal (0-5V logic) output from the comparator produces a glitch that can be seen on the corresponding channel. This effect is seen in the channel with the injected charge, as well as, to a lesser extend, in the first neighboring channels.

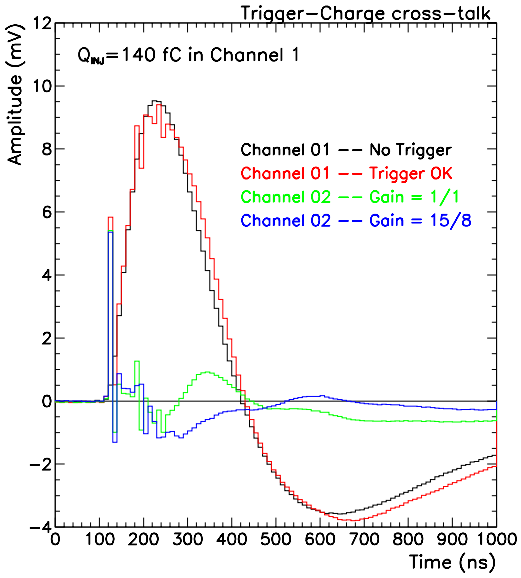

Figure 3.37: *Effects seen on a charge channel due to the trigger-charge couplings*

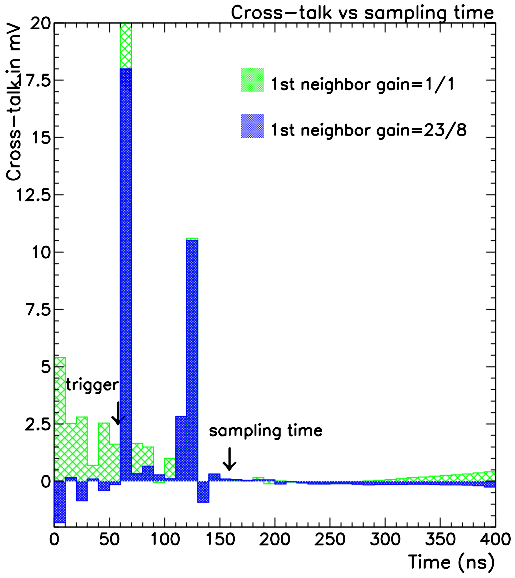

Figure 3.38: *Trigger-Charge cross-talk as function of the time of the slow shaper signal storage*

The magnitude of this effect does not affect significantely the charge measurement. Indeed, upon a trigger decision, the slow shaper signal sampling occurs after about 100 ns, time at which the

cross-talk magnitude has to be assessed. This is done in Fig. 3.38 which shows the magnitude of the distortion as function of the charge sampling time. Such effect amounts for less than 1 mV, which corresponds to 5% of photoelectron maximum. This effect does not show any sizeable depence on the gain correction settings, as seen in the first neighboring channel in Fig. 3.38. This additionnal peak up signal seems to be a coupling between the comparator output and somewhere after the preamplifier as this phenomenon is independant of the weights applied to the channel with no input. One notices also some influence due to the mask of the channel which receives the input signal. The exact origin of the coupling is probably due to power supply glitch to the comparator.

3.4.2 Charge-Charge crosstalk

Couplings between neighboring channels is also a cause of cross-talk. This coupling depends on the geometry and location of the tracks on the chip, as it is is displayed in Fig. 3.39 and Fig. 3.41.

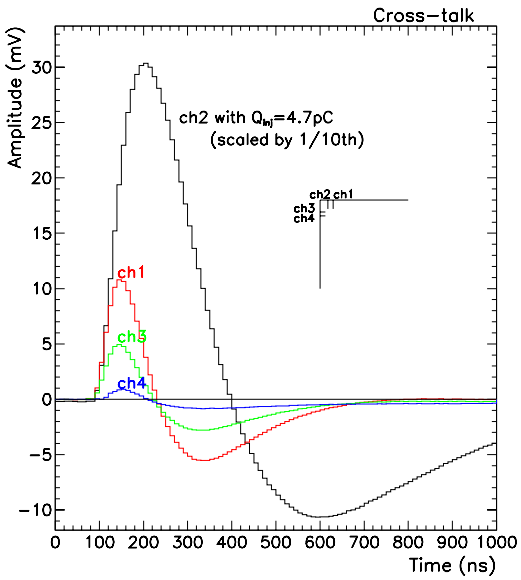

Figure 3.39: *Cross-talk measured between the first two neighboring channel. Mind the 1/10th scale for the channel with the injected charge*

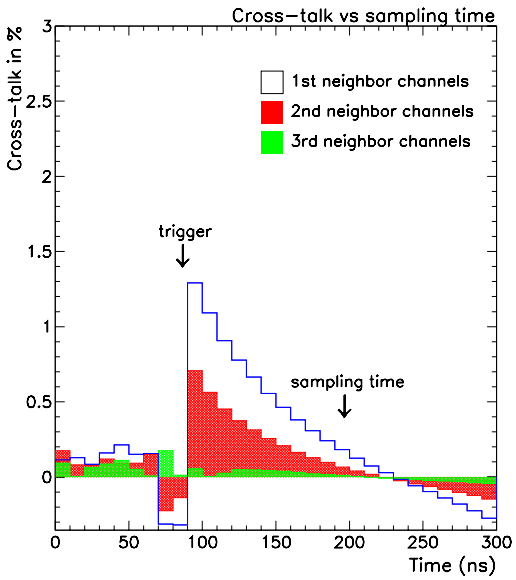

Figure 3.40: *Close up of the cross-talk signals in first and 2nd neighbors as function of the sampling time. Numbers are in percent*

The waveform output of a channel with an injected charge of 0.45 pC (3 p.e.) is compared to adjacent channel outputs. It appears that only the first and second neighbor channels are affected by the fired channel. As previously, what matters is the cross-talk magnitude at the sampling time, around 100 ns. At this time, the measured channel-to-channel cross-talk is of the order of 0.5% for the 1st neighbor and well below 0.1% for the 2nd neighbor. Fig. 3.40 and

3.42 show the dependence of this cross-talk magnitude as function of the sampling time in a window centered around 100 ns. In all cases, this cross-talk does not affect charge measurement significantely, compared to cross-talk values measured at the multi-anode PMT stage. In this latter effects can reach 4-5% as shown in [5].

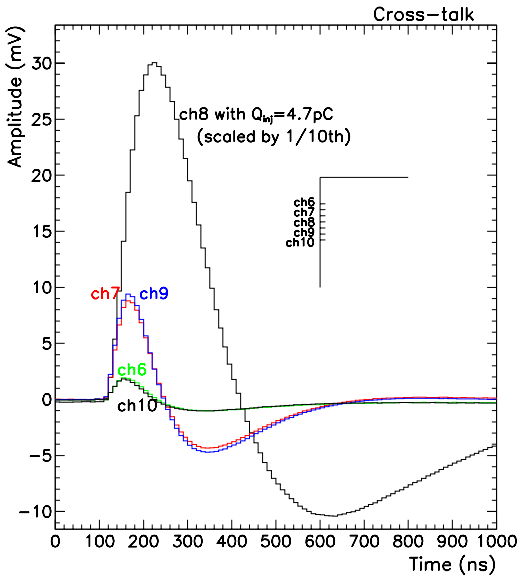

Figure 3.41: *Cross-talk measured between the first two neighboring channel. Mind the 1/10th scale for the channel with the injected charge*

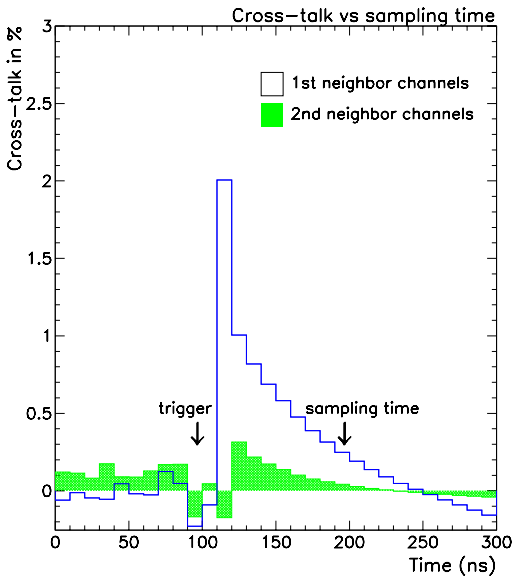

Figure 3.42: *Close up of the Cross-talk as function of the sampling time. Numbers are in percent*

3.5 Electronic noise for slow and fast shapers

Electronic noise has also been measured using an external shaper, with adjustable peaking time by measuring the distribution of pulse heights for a fixed charge injected to the input. The charge equivalent noise is then given by ENC = $Q_{inj} \times \frac{\sigma_{(rms)}}{V_{max}}$. Noise is found to remain below 1% of photoelectron at t_P =30 ns corresponding to the fast shaper, as shown in Fig.3.43. It also appears below 2% of photoelectron at 100 ns peaking time, which makes the chip perfectly suitable for the TT requirements as recalled in Section1.

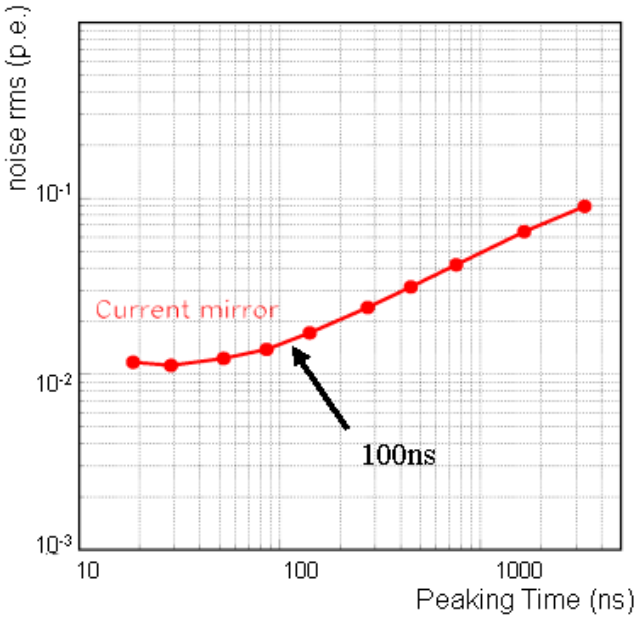

Figure 3.43: *(Charge equivalent) Noise RMS in photoelectron as measured for the shapers. Slow shaper functions at 30 ns, fast shaper at 100 ns*

3.6 Multiplexing and Mask

Test results performed at Bern and LAL show no problem. The output level is around 3V for the maximum amplitude. In the present design, noisy channel cannot be switched OFF. Instead, there is a mask at the trigger level (AND after the comparator) that allows to avoid triggering on the noisy channel. The readout is clocked at 5MHz and it takes 6.4μs to read the 32 channels (in serie).

4 Summary

4.1 Performance

Table 1 reports the performance as measured on the 32 channel chip. The Version 2 chip performance suit the Target Tracker requirements. A 100% trigger efficiency is ensured down to 1/3rd photoelectron, the linearity in the charge measurement is ensured in the [1-80] photoelectron range with a response linearity better than 1% up to 75 photoelectrons, and the gain correction at the preamplifier stage has been proved fully functionnal. This ASIC can thus be considered as a working version fullfilling the Target Tracker requirements, as defined by the collaboration.

Auto-Trigger:	
- Fast shaper peak time	$t_p = 30$ ns
- Fast shaper Gain	880 mV/pC (140 mV/p.e)
- Comparator Threshold Spread	15 mV (0.05 p.e.)
- Noise RMS	1.5-4.0 mV ($<<$ 1 pe)
Charge Measurement:	
- Dynamic range	[0-13 pC] (75 p.e)
- Slow shaper peak time	$t_p = 105$ ns
- Slow Shaper Gain	133 mV/pC (21 mV/p.e)
- Pedestal Spread	$\pm$15 mV (1 p.e.)
- Noise RMS	1.5 mV
- Gain Correction	1 to 2.875 (4 bits)
- Track & Hold	Operational
- Cross-talk	$\mathcal{O}(1\%)$
Multiplexing	Operational (3V max. output)
Clock frequency	5 MHz (6.4μs/32channels)
Mask of noisy channel	Trigger Level
Trigger signal	Comparator output
Tag of the triggered channel	Not included

Table 1: *Functionalities of the 32-channel chip*

4.2 Costs estimates

The cost for a multiproject including 15 units (produced, packed and encapsulated) is $\approx$ 5.2 kEuros. This estimate is basically unchanged from Version 1a to Version 2 since it mainly depends

	Nb of ASIC units	Cost per channel	Total Cost
Version 2 (test)	15	10.8 euros	5.2 keuros
Version 2 (full prod.)	2000	0.7 euros	46.0 keuros

Table 2: *Cost of the ASICs designed at LAL*

on the chip area, which remains basically identical. The cost estimate for a full production based on 2000 ASIC's is about 46 kEuros. All numbers are reported in Table 2.

4.3 Conclusion

The FE electronic ASIC designed and tested by both LAL and Bern Group is found to suit the Target Tracker requirements: the preamplifier stage is proven to be functional and allow to correct for input non-uniformity of about 2.875 with a good precision; the auto-trigger functionality has been tested and found to be 100% efficient at a 1/3rd of photoelectron with a negligible electronic noise; the charge measurement feature has been proven reliable over the [0-90] photoelectron dynamic range, with a response linearity better than 1% up to 75 photoelectrons. Systematic checks have been performed and show that effects such as cross-talks have no impact on physics measurements. We conclude that this version satisfies the Target Tracker requirements.
Another version is currently under testing. This upgrade version is expected to further improve several aspects of the current Version-2, with reduced pedestals, smaller electronic noise and cross-talks and with an extended dynamic range. A report will be released soon.

References

[1] OPERA Proposal, CERN/SPSC 2000-028, SPSC/P318, LNGS P25/2000 and "Status Report on the OPERA experiment", CERN/SPSC 2001-025, SPSC/M668, LNGS-EXP 30/2001

[2] M.Dracos et al., "Plastic sintillator target tracker proposal and studies done at Strasbourg", OPERA-NOTE 26, 16 June 2001.

[3] CERN Finance Comittee, 290th meeting, 19 June 2002 CERN/FC/4583

[4] R. Arnold, E. Baussan et al, IReS, "Results about H7546 Multianode PMT's studies", OPERA Note 30,

[5] S. Monteil, and private communication. LHCb talk.

[6] M. Dracos, private communication

[7] "Performance of the 32-channels FE electronics for the OPERA Target Tracker", Opera-note 34

[8] C. de La Taille, G. Martin-Chassard, L. Raux, LAL Orsay, presentations at OPERA Target Tracker meetings, CERN Jul-2001, CERN October 10-2001, CERN Fevrier-2002 accessible on http://www.lal.in2p3.fr/recherche/opera/internal_hard.html